Chapter 6
Designing and Understanding Building Blocks for Molecular Spintronics

Carmen Herrmann, Lynn Groß, Bodo Alexander Voigt, Suranjan Shil and Torben Steenbock

Abstract Designing and understanding spin coupling within and between molecules is important for, e.g., nanoscale spintronics, magnetic materials, catalysis, and biochemistry. We review a recently developed approach to analyzing spin coupling in terms of local pathways, which allows to evaluate how much each part of a structure contributes to coupling, and present examples of how first-principles electronic structure theory can help to understand spin coupling in molecular systems which show the potential for photo- or redoxswitching, or where the ground state is stabilized with respect to spin flips by adding unpaired spins on a bridge connecting two spin centers. Finally, we make a connection between spin coupling and conductance through molecular bridges.

6.1 Introduction

In electronics on a very small scale, heating due to electron currents flowing through thin wires has become a major problem [1]. In spintronics, information is stored, transferred and processed employing the spin rather than the charge degree of freedom. Spintronics offers, in principle, a solution to the heating challenge: By building up chains of spins which are coupled to their neighbors by (super-)exchange or by Ruderman–Kittel–Kasuya–Yosida (RKKY) interactions (when adsorbed on a metal surface), the flip of a spin on one end of the chain can be passed on along the chain, thus transferring information but not charge. This has been exploited in an experiment by Khajetoorians et al. [2], in which it was demonstrated that chains of iron atoms deposited on a copper substrate can be used to build a spin logic gate. The inputs are controlled by cobalt clusters of different size whose magnetization can be individually switched by an external magnetic field due to their different coercivities, and the output is read out by the tip of a spin-polarized scanning tunneling microscope

C. Herrmann (✉) · L. Groß · B. A. Voigt · S. Shil · T. Steenbock
Institute for Inorganic and Applied Chemistry, University of Hamburg, Martin-Luther-King-Platz 6, 20146 Hamburg, Germany
e-mail: carmen.herrmann@chemie.uni-hamburg.de

R. Wiesendanger (ed.), *Atomic- and Nanoscale Magnetism*, NanoScience and Technology, https://doi.org/10.1007/978-3-319-99558-8_6

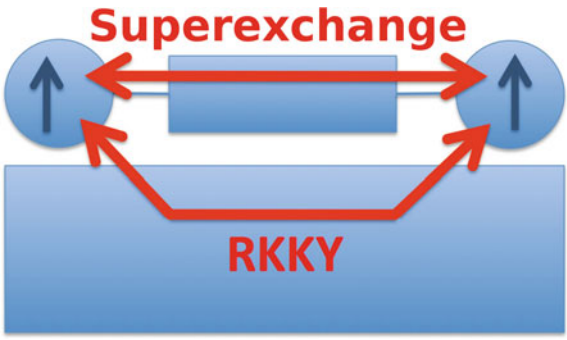

Fig. 6.1 Schematic representation of two spin centers (e.g., metal atoms) linked by a ligand adsorbed on a surface, with two possible competing spin–spin interactions

(STM). The atoms are coupled antiferromagnetically by RKKY interactions mediated by the conduction electrons. Controlling this interaction requires controlling the distance between the atoms on the surface, which is achieved by manipulating them with the STM tip. A simpler approach to constructing spin chains is provided by molecular self-assembly on surfaces. Molecules consisting of spin-polarized metal ions and organic ligands can be covalently linked into antiferromagnetically coupled chains and branched structures by thermally activated surface-mediated debromination [3–5]. Chain lengths of up to 81 nm could be achieved [5]. Linking metal atoms via ligands in this way introduces two competing pathways for spin coupling: one is through the surface (RKKY) and one through the bridging ligand(s) (see Fig. 6.1). To find out which of these two dominates, one usually resorts to density functional theory (DFT) calculations, comparing spin coupling for pairs of molecules on the substrate with pairs of molecules in the vacuum. In the covalently linked molecular chains discussed above, this procedure suggested that spin coupling is mediated solely through the ligands [3]. For a checkerboard structure of molecular spin centers whose ligands were *not* covalently linked to each other, the same approach suggested that only RKKY interactions are responsible for spin coupling [6]. For similarly non-linked charged tetracyano-*p*-quinonedimethane molecules adsorbed on graphene/Ru(0001), in contrast, interactions between the molecules rather than the substrate were suggested as being responsible for spin interactions [7].

Taking away the substrate will not strongly modify the electronic structure of the adsorbed molecule if molecule–substrate interactions are sufficiently weak. For cases where these interactions affect the electronic structure of the adsorbate and for the sake of efficiency, it is desirable to have a computational scheme which allows to evaluate the dominant coupling pathway more directly. Such a scheme is also helpful for disentangling the different contributions to spin coupling that may arise *within* a given molecule (e.g., because different bridging ligands are present). In Sect. 6.2.2, such a local decomposition scheme is presented [8]. It is based on a Green's function approach to evaluating spin coupling from the electronic structure of one spin state only (rather than from energy differences between two spin states) which has been established in solid-state science [9] and only occasionally been applied to molecules [10–12] (with spin densities clearly localized on the metal atoms

rather than partially delocalized onto ligands). Therefore, it had to be ensured that the approach works generally well for molecules [13]. For this purpose, it was brought into a form suitable for interfacing with quantum chemical electronic structure codes [13] based on previous work by Han, Ozaki and coworkers [12]. Both is summarized in Sect. 6.2.1.

As an additional advantage, spin coupling between or within molecules can be controlled chemically to a large degree. The term "chemical control" can refer to optimizing molecular bridges and/or spin centers in terms of chemical constitution, substituents and molecular topology, and to constructing structures that can be switched by external stimuli, thus modifying spin coupling by, e.g., illumination with visible or ultraviolet light [14–19]. We discuss a candidate for such photoswitching of spin coupling in Sect. 6.3.1, and elucidate, with the help of DFT calculations, possible reasons for the unfavorable switching behavior of the complex. In Sect. 6.3.2, an alternative switching mechanism is discussed: a ferrocene unit bridging two organic radicals is oxidized, so that an additional unpaired spin on the bridge is introduced. As for the photoswitching in the example above, this does not affect the type of spin coupling (i.e., there is no change between ferro- and antiferromagnetic coupling), but it strongly changes its magnitude (i.e., the energy difference between the ferro- and antiferromagnetically coupled states). Such oxidation switching of spin coupling has also been studied experimentally and theoretically for different types of bridges [20–22]. The effect of oxidation may also be relevant, for example, when comparing isolated molecules with molecules adsorbed on surfaces, as the interaction with a metal substrate may lead to charge transfer between molecule and surface. To isolate the effect of an additional spin on the bridge from the effect of charging, a comparative study on neutral bridges with and without unpaired spin is finally presented in Sect. 6.3.3, which points to achieving delocalization of the spin density onto the bridge as a major goal for synthetic efforts towards molecules or molecular chains with large spin coupling. Introducing spin on the bridge as a means to achieve larger spin coupling has gained increase interest in recent years [23].

The logic gate described above operates at a temperature of 0.3 K. Employing molecules and optimizing their interactions may lead to devices with higher operating temperatures. At the same time, these potential technological applications are by far not the only reason why we are interested in understanding and designing spin interactions within and between molecules. Such spin interactions are important, e.g., for catalysts and biological systems, and ligands mediating them may be understood as a specific example of communication through molecular bridges, which is also relevant for, e.g., electron transfer and transport through such bridges [24–30]. Section 6.4 summarizes several examples of how first-principles electronic structure calculations can help to draw analogies between spin coupling and conductance, and to understand conductance in cases where spin plays an important role.

6.2 Local Pathways in Exchange Spin Coupling

In contrast to various properties such as charge [31, 32], spin [33–35], electric dipole moments [36–38], electron transport and transfer properties [39–46], Raman or vibrational Raman optical activity intensities [47, 48], and X-ray absorption intensities [49, 50], there is no straightforward scheme available for analyzing which parts of a molecular structure contribute to coupling between local spins. We present here such a scheme, based on a Green's function approach from solid-state physics [9].

6.2.1 Transferring a Green's Function Approach to Heisenberg Coupling Constants J from Solid State Physics to Quantum Chemistry

In quantum chemistry, the coupling between spin centers is usually evaluated from the energy difference between a ferromagnetically coupled and an antiferromagnetically coupled state (see Fig. 6.2). If one assumes a cosine dependence of the electronic energy on the angle between the two spin vectors located at the spin centers (see Fig. 6.2), one can estimate this energy difference by looking at the electronic structure of one spin state only: as illustrated in Fig. 6.2, the larger the energy difference, the larger the curvature of the energy at one of the extrema corresponding to ferro- or antiferromagnetic coupling. This was the basis for the approach developed for solid-state structures [9]. We have checked whether the energy does indeed show such a cosine behavior and found that as long as the spin does not strongly delocalize onto the bridge, with bridge atoms sharing delocalized spin from different spin centers, this is usually the case [13]. Of course, differences in molecular orbitals (MOs) and molecular structures in different spin states are neglected by such an approach. Nonetheless, it was found to give reliable spin couplings for a wide range of structures. Compared to an approach by Peralta and coworkers [51, 52], in which orbital relaxation upon spin rotation is taken into account by solving the coupled perturbed Kohn–Sham equations, the Green's function approach sacrifices some accuracy for the advantage of being a straightforward postprocessing scheme.

If magnetic anisotropy is low, spin coupling is usually well described by a Heisenberg Hamiltonian

$$\hat{H} = -2J \sum_{A>B} \hat{\mathbf{S}}_A \cdot \hat{\mathbf{S}}_B, \tag{6.1}$$

where J refers to the spin coupling constant (which is positive for ferromagnetic and negative for antiferromagnetic coupling), and $\hat{\mathbf{S}}_A$ and $\hat{\mathbf{S}}_B$ to the local spin operators for spin centers A and B. By comparing the energy change due to a small spin rotation between a Greens-function energy expression and the Heisenberg model, using the local force theorem, and introducing local projection operators onto the spin

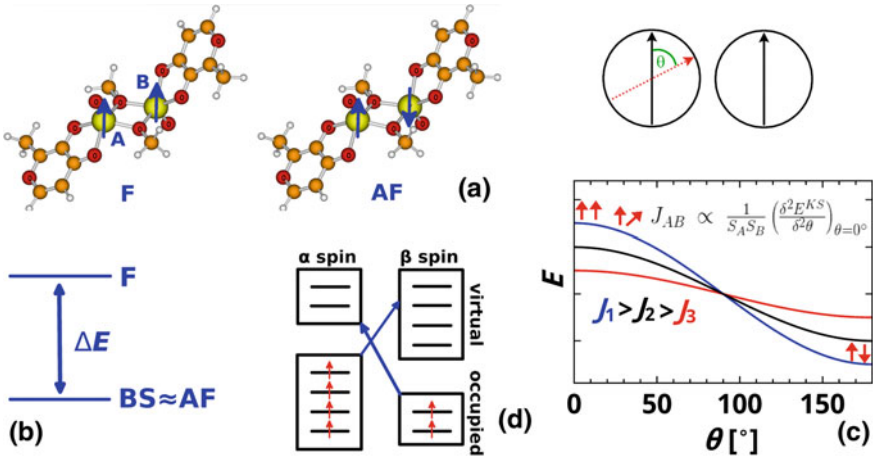

Fig. 6.2 The standard approach to evaluating spin coupling in quantum chemistry is based on evaluating energy differences between ferromagnetically (F) and antiferromagnetically (AF) coupled states (**a**), where the AF state is typically modeled by a Broken-Symmetry (BS) determinant in Kohn–Sham DFT (**b**). In the approach from solid-state physics adopted here, spin coupling is rather evaluated from the curvature of the potential energy as a function of the angle θ between two local spin vectors (**c**). The larger the energy difference, the larger the curvature. The resulting expression involves sums over pairs **d** of occupied spin-up or α orbitals and unoccupied spin-down or β orbitals, or vice versa ("spin-flip excitations"; compare (6.2)).

centers to define so-called on-site potentials, we arrive at the following equation for J (evaluated by processing the electronic structure of the ferromagnetically coupled state),

$$
\begin{aligned}
J(\mathrm{F}) = &-\frac{1}{4S_A S_B} \sum_{\substack{i\in\mathrm{occ}\\ k\in\mathrm{virt}}} \sum_{\substack{\{\mu,\nu\}\in A\\ \{\mu',\nu'\}\in B}} C^{\alpha}_{\nu i} \left(F^{\alpha}_{\mu\nu} - F^{\beta}_{\mu\nu}\right) C^{\beta *}_{\mu k} \\
&C^{\alpha *}_{\mu' i} \left(F^{\alpha}_{\mu'\nu'} - F^{\beta}_{\mu'\nu'}\right) C^{\beta}_{\nu' k} \frac{1}{\epsilon^{\alpha}_i - \epsilon^{\beta}_k} \\
&-\frac{1}{4S_A S_B} \sum_{\substack{k\in\mathrm{occ}\\ i\in\mathrm{virt}}} \sum_{\substack{\{\mu,\nu\}\in A\\ \{\mu',\nu'\}\in B}} C^{\alpha}_{\nu i} \left(F^{\alpha}_{\mu\nu} - F^{\beta}_{\mu\nu}\right) C^{\beta *}_{\mu k} \\
&C^{\alpha *}_{\mu' i} \left(F^{\alpha}_{\mu'\nu'} - F^{\beta}_{\mu'\nu'}\right) C^{\beta}_{\nu' k} \frac{1}{\epsilon^{\beta}_k - \epsilon^{\alpha}_i}, \\
= &\sum_{ik} j(i,k).
\end{aligned}
\tag{6.2}
$$

For a detailed derivation, see [9, 13]. The sums run over pairs of occupied and unoccupied ("virtual") orbitals of opposite spin and over single-particle basis functions

μ, ν located on the spin centers A and B. $F^{\sigma}_{\mu'\nu'}$ refers to the elements of the Fock matrices for electrons of spin $\sigma \in \{\alpha, \beta\}$, where α refers to spin-up or majority spins and β refers to spin-down or minority spins, in a basis of Löwdin-orthogonalized atom-centered single-particle basis functions. In other words, this is a matrix representation of the effective single-particle operators in Kohn–Sham DFT. $C^{\sigma}_{\nu i}$ denotes the molecular orbital coefficients for a given spin σ in the same basis. S_A and S_B refer to the local spin quantum numbers on the spin centers A and B. So far, we have used ideal local spin quantum numbers rather than the local spins $\langle \hat{S}_{zA} \rangle = \frac{1}{2}(N^{\alpha}_A - N^{\beta}_A)$, where N^{σ}_A is the number of electrons with spin σ on atom A.[1]

In our case, Löwdin projectors were used [31, 53, 54], but other choices, may have their benefits as well (e.g., local partitioning schemes based on three-dimensional Cartesian space rather than on single-particle basis functions)—compare the long list of methods for analyzing partial atomic charges (population analysis). It should also be noted that there is a certain ambiguity in defining the on-site potentials (which reflect the difference in potential a spin-up electron experiences on an atom compared with a spin-down electron) in terms of local projection operators. This is discussed in more detail in [13] and shown to not strongly affect the resulting coupling constants. In all cases considered here, the two spin centers were chosen as the two atoms on which the unpaired spins are formally located (i.e., the metal atoms). In particular in strongly delocalized systems such as organic radicals, including more atoms can be advisable.

If the electronic structure of the antiferromagnetically coupled state was employed, an expression equivalent to (6.2) would be obtained, except for a sign change ($J(\mathrm{AF}) = -J(\mathrm{F})$). In Kohn–Sham DFT, the wave function of the noninteracting reference system in the antiferromagnetically coupled state is usually modeled by a so-called Broken-Symmetry determinant [55], which breaks spin symmetry. There is some debate in the literature on whether this is formally correct [56–59], in particular since it is not clear how to evaluate the total spin in Kohn–Sham DFT [60, 61]. In practice, the Broken-Symmetry approach has been very successful in modeling molecular structures and energetics of antiferromagnetically coupled systems [56, 62], and whether spin projection is considered necessary or not typically has a much smaller effect on the resulting J than the choice of approximate exchange–correlation functional. We found that when applied to a Broken-Symmetry determinant in Kohn–Sham DFT, the Green's function approach ((6.2) with a sign change) does not even consistently produce qualitatively reliable coupling constants (see Fig. 6.3). Figure 6.3 shows data for two transition metal complexes which are particularly challenging, as the unpaired spin is partially delocalized from the metal atoms onto the ligands.

The lower panels of Fig. 6.3 also illustrate the challenge resulting from structural differences in the minimum-energy structures in the two spin states: depending on which molecular structure is chosen, the sign of the predicted coupling constant

[1] Ideal local spin quantum numbers would be $S_A = \frac{1}{2}$ for a spin center with formally one unpaired electron, while local spins reflect the decrease of this number that results from delocalization of unpaired spin density onto neighboring atoms such as ligands.

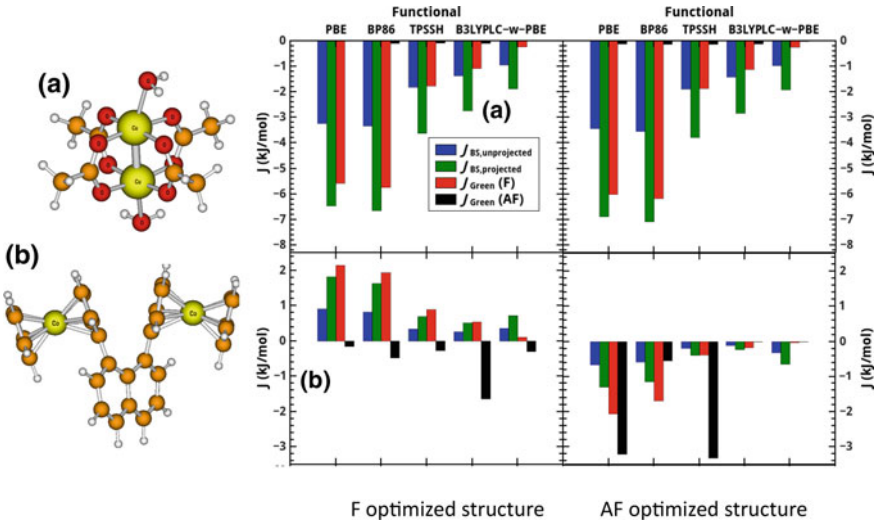

Fig. 6.3 Exchange coupling constants J for a $[Cu_2]$ (top) and a bis-cobaltocene complex (bottom), which show non-negligible delocalization of spin density from the metal atoms onto the ligands [13]. J is evaluated employing either the "traditional" energy-difference method between a ferromagnetically coupled and a Broken-Symmetry (BS) determinant with or without spin projection, or from (6.2) based on a ferromagnetically (F) or antiferromagnetically coupled (AF) electronic structure. The molecular structures were optimized either in the F state (left) or in the AF state (right). Different approximate exchange–correlation functionals were used (see x axis) in combination with a def-TZVP basis set. The experimental data are $J = -1.54$ kJ/mol for $[Cu_2]$ [63] and $J = -0.33$ kJ/mol for bis-cobaltocene [64]. In other words, for the bis-cobaltocene a prediction of the spin multiplicity of the ground state is not possible with the Green's function approach employing the chosen DFT settings. This is, however, the only case we have encountered so far in which J was this sensitive to the electronic structure

changes. This was the only case observed in our studies so far, but it would clearly be valuable for future work to establish a reliable measure or rule for when such structural differences play a role.

6.2.2 *Decomposing J into Local Contributions*

Equation (6.2) consists of sums over pairs of occupied spin-up (or α) and unoccupied spin-down (or β) orbitals, or vice versa (see Fig. 6.2d). These may be considered as "spin-flip excitations" $j(i, k)$,

$$j(i,k) = \frac{q}{4S_A S_B} \sum_{\substack{\{\mu,\nu\}\in A \\ \{\mu',\nu'\}\in B}} C^{\alpha}_{\nu i} \left(F^{\alpha}_{\mu\nu} - F^{\beta}_{\mu\nu}\right) C^{\beta *}_{\mu k}$$
$$C^{\alpha *}_{\mu' i} \left(F^{\alpha}_{\mu'\nu'} - F^{\beta}_{\mu'\nu'}\right) C^{\beta}_{\nu' k} \frac{1}{\epsilon^{\alpha}_i - \epsilon^{\beta}_k}, \tag{6.3}$$

where i refers to the index of an α orbital and k to the index of a β orbital. The factor q is equal to 1 if i is occupied and k unoccupied, and -1 if i is unoccupied and k occupied. For pairs of occupied or unoccupied orbitals, q is zero. These molecular orbitals are often predominantly localized on a certain part of a molecular structure, for example on a certain bridging ligand or on one or several spin centers. This suggests to employ these spin-flip excitations directly for the analysis of local contributions to spin coupling pathways. This is not straightforward, since the individual $j(i,k)$ make large contributions of opposite signs, which then barely cancel to result in the total coupling constant. This is analyzed in detail for the H_2 molecule in [8].

As an alternative, one can focus on, e.g., the occupied MOs, and sum over all spin-flip excitations from each occupied MO,

$$j^{\alpha}_{\mathrm{MO}}(i) = \sum_{k\in\beta,\mathrm{virt}} j(i,k) \tag{6.4}$$

$$j^{\beta}_{\mathrm{MO}}(k) = \sum_{i\in\alpha,\mathrm{virt}} j(i,k) \tag{6.5}$$

so that

$$J\,(\mathrm{F}) = \sum_{i\in\mathrm{occ},\alpha} j^{\alpha}_{\mathrm{MO}}(i) + \sum_{k\in\mathrm{occ},\beta} j^{\beta}_{\mathrm{MO}}(k). \tag{6.6}$$

Other choices such as focusing on, e.g., all α orbitals (occupied or unoccupied) would be equally valid in principle. One argument for selecting occupied MOs of both spins would be that these are variationally optimized, while the virtual orbitals are not (except for being orthogonal to the occupied ones). These MO contributions are typically much smaller in absolute value than the (nearly canceling) spin-flip excitations they are constructed from, so that they appear to be a more reasonable choice for further analysis.

One can then proceed as follows: First, the most important contributions j^{σ}_{MO} from occupied orbitals are selected (with a cutoff chosen either as a certain percentage of J, or as an absolute value). Then, the largest spin-flip excitations contributing to those can be analyzed further. The advantage of such an orbital-based approach is that it can generate insight in terms of orbital symmetry. There is often some ambiguity in deciding which orbital resides on which part of the structure, so that this scheme is not ideally suited for an automated decomposition. Also, if one is predominantly interested in contributions from different atom-centered basis functions on the spin centers (in particular those corresponding to d orbitals on the metal atoms),

an alternative scheme in which the individual terms resulting from the double sum over the basis functions located on the spin centers in (6.2) are analyzed may be more promising [65, 66].

A more straightforward scheme for analyzing the contributions of different regions of space to spin coupling is an atomic decomposition, which can be based on defining weights of each molecular orbital i of spin σ on an atom or molecular fragment A,

$$\omega_A^\sigma(i) = \frac{\sum_{\mu \in A} \left| C_{\mu i}^\sigma \right|^2}{\sum_\nu \left| C_{\nu i}^\sigma \right|^2}, \tag{6.7}$$

$$\sum_A \omega_A^\sigma(i) = 1, \tag{6.8}$$

(where $C_{\nu i}^\sigma$ again refers to MO coefficients w.r.t. a Löwdin-transformed basis) and then defining a fragment contribution to J such that the spin-flip excitations are weighted according to the average weight of the two orbitals involved on the fragment under consideration,

$$j_{\text{Frag}}(A) = \sum_{i,k} \left(\frac{\omega_A^\alpha(i) + \omega_A^\beta(k)}{2} \right) j(i,k), \tag{6.9}$$

$$J(\text{F}) = \sum_A j_{\text{Frag}}(A). \tag{6.10}$$

Again, there is some degree of arbitrariness in this approach, and one might, for example, consider a density-based weighting scheme in future work, or taking the geometric rather than the arithmetic average between the two fragment weights. From our experience so far, the approach described above works well for the purpose of qualitative analysis we have in mind (see below and [8]).

The calculation and local decomposition of exchange coupling constants J was implemented in our program package ARTAIOS [67] (see Fig. 6.4), which can post-process output from various electronic-structure codes.

6.2.3 *Application to Bismetallocenes: Through-Space Versus Through-Bond Pathways*

As an illustrative example, we show here the analysis of through-bond versus through-space coupling pathways for naphthalene-bridged bis-metallocenes synthesized by Heck and coworkers [68, 69] (see Fig. 6.5).

We compare the fragment decomposition scheme according to (6.7)–(6.10) with an alternative approach, in which the bridge is removed to evaluate the pure through-space contribution (see Table 6.1). As discussed in the introduction, this has the

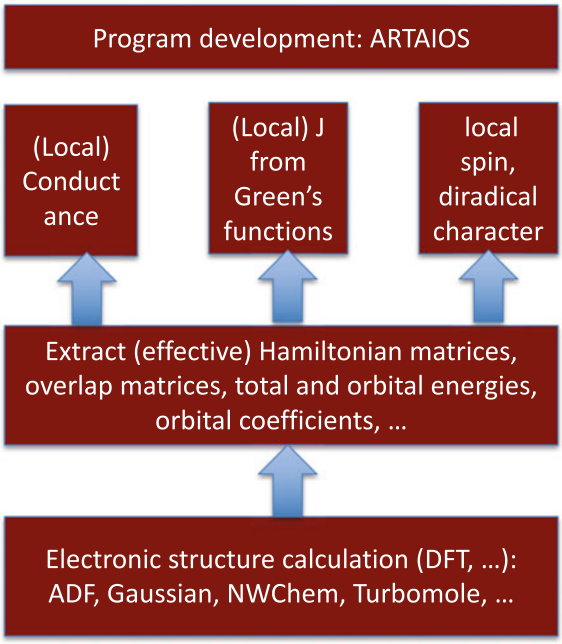

Fig. 6.4 Schematic workflow in our program package ARTAIOS [67]

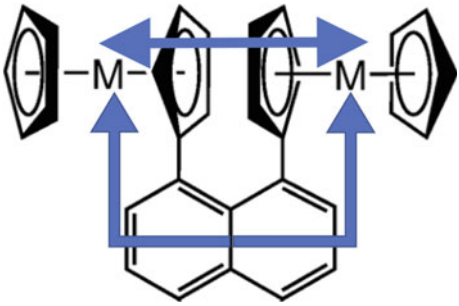

Fig. 6.5 Illustration of two spin coupling pathways in bis-metallocenes (top: through-space, bottom: through-bond)

disadvantage of modifying the electronic structure of the spin centers somewhat, so that removing the bridge may also modify the through-space interactions to some extent. Qualitatively, both approaches result in the same picture: For vanadocene, the overall coupling is weak because both pathways contribute little (which can be attributed to the small delocalization of unpaired spin from the spin centers onto the ligands [69]), while for nickelocene, the antiferromagnetic coupling is dominated by the through-space interaction (with the bridging contributing a smaller equally antiferromagnetic term).

Table 6.1 Through-space (TS) and through-bond (TB) contributions to the Heisenberg spin coupling constant J (in cm^{-1}) for naphthalene (NP)-bridged bis-cobaltocenes. The values in the second column were obtained by evaluating H for a molecule in which the bridge was taken out and replaced by two hydrogen atoms to saturate the dangling bonds (but all other nuclear coordinates were the same as in the molecule including the bridge; see Fig. 6.6). For the values in the third column, the resulting J was subtracted from J for the full molecule (including the bridge). In all calculations TPSSH / def2-TZVP was used

System	TS (no bridge)	TB (total − no bridge)	TS (6.9)	TB (6.9)
V–NP–V	−0.2	−0.2	−1.2	+0.7
Ni–NP–Ni	−24.3	−1.3	−17.3	−8.3

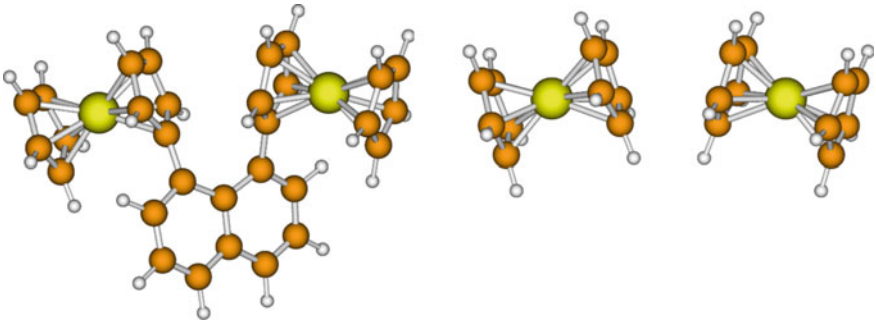

Fig. 6.6 Ball-and-stick representation of a bis-metallocene with and without a naphthalene bridge (in the structure without the bridge, the dangling bonds are saturated with hydrogen atoms)

6.3 Chemically Controlling Spin Coupling

In the ideal case, chemical control can be exerted by external stimuli, e.g., by modifying the chemical structure of a bridge between two spin centers through photo- or redoxswitching. Nonetheless, comparing different bridges that are not directly interconvertible, as presented in the last part of this section, is very helpful for establishing structure–property relationships.

6.3.1 Photoswitchable Spin Coupling: Dithienylethene-Linked Biscobaltocenes

Bismetallocenes with dithienylethene (DTE) linkers promise a combination of photo- and redox-switching, and for metallocenes with unpaired electrons, photoswitchable spin coupling. This has been demonstrated for DTE-linked organic radical spin centers, and occasionally also between metal centers [70]. Attempts at bringing a cobaltocene–DTE-cobaltocene molecule (see Fig. 6.8, top right), where each cobal-

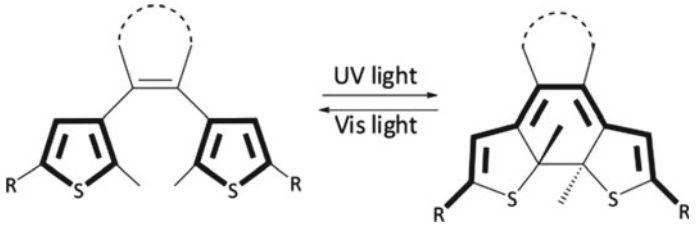

Fig. 6.7 Photoswitching a dithienylethene bridge with different substituents R. π-conjugation is indicated by the thick lines. The dotted line indicates one or two methylene units, resulting in five-membered and six-membered rings, respectively, which were both studied without showing much difference in their switching behavior

tocene carries one unpaired spin, to photoswitch between an uncoupled "open" and a coupled closed form were not successful [19]. By studying a sequence of disubstituted dithienylethene bridges and comparing their switching behavior with ground- and excited-state potential energy (PES) scans along the reaction coordinate, we could shed some light on why this is so.

For chlorine-substituted DTE, photoswitching is possible, and this is true for both a five-membered and a six-membered ring [71]. The advantage of a six-membered ring is its potential for chiral functionalization. When attaching (diamagnetic) ferrocene substituents for R in Fig. 6.7, the switching behavior was considerably poorer than for the chlorine-substituted compound. This could be attributed to an increased number of accessible excited electronic states, only one of which results in the desired photoreaction [72]. This increased number of excited-state pathways not leading to ring closure or opening is even more pronounced when moving to a DTE bridge with two attached paramagnetic cobaltocene units. This is in contrast to the case where the π systems of substituents and bridge are disconnected by a sp^3-hybridized carbon atom (see Fig. 6.8). Accordingly, while the latter system can be photoswitched, it was not possible to switch the corresponding bis-cobaltocene [19].

6.3.2 Redox-Switchable Spin Coupling: Ferrocene as Bridging Ligand

Ferrocene was mentioned above as a substituent on a photoswitchable bridge. Here, we exploit its redox properties and employ it as a bridge between two radical substituents (see Fig. 6.9). In the neutral state, ferrocene is diamagnetic, while in the oxidized state, it has one unpaired electron. This unpaired electron can interact with the unpaired electrons on the two radical substituents, so that one would expect an increase in overall spin coupling (i.e., energy difference between the electronic ground state and excited states obtained by spin flips). This is indeed the case: In the neutral form, the spins on the radical substituents are weakly ferromagnetically

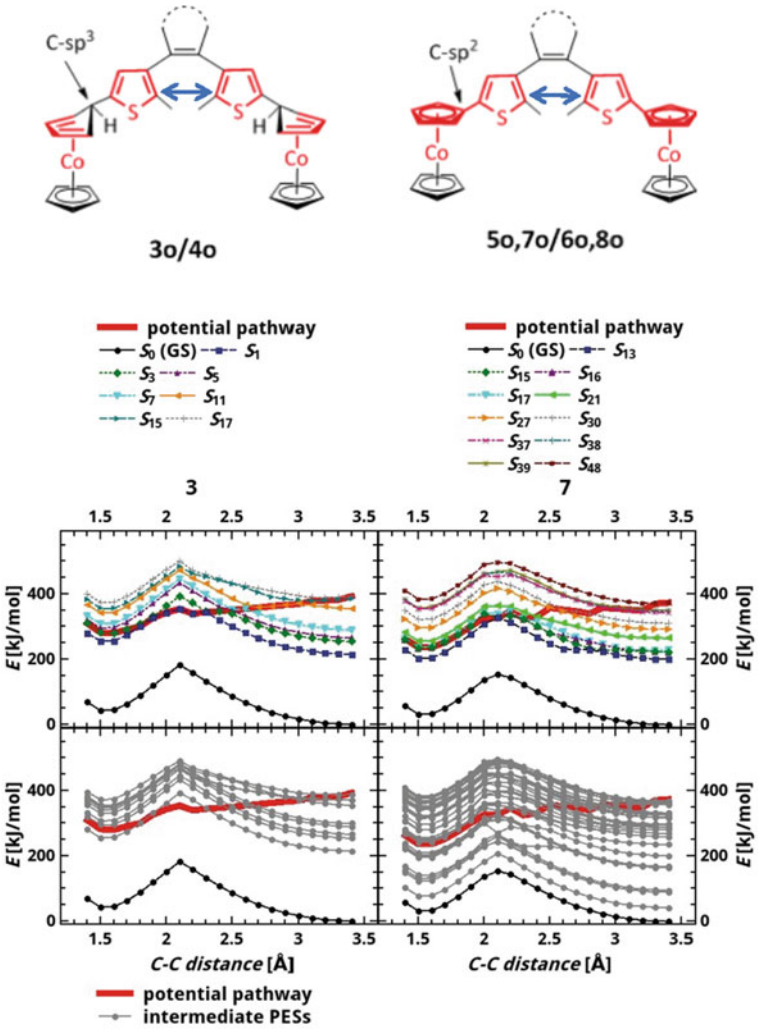

Fig. 6.8 Top: Lewis structures of DTE-linked complexes with diamagnetic Co(I) centers attached via sp^3-hybridized carbon atoms (left) and with paramagnetic cobaltocene (Co(II) centers attached via sp^2-hybridized carbon atoms, resulting in π conjugation between DTE and the cyclopentadienyl ligands (right). The dotted line indicates one or two methylene units, which were both studied without showing much difference in their switching behavior. The data shown below are for the five-membered ring resulting from one methylene unit. Middle: Total energy as a function of the distance between the reactive carbon atoms involved in ring closure / opening (indicated by the blue arrows in the top panels), for the ground state and for those excited states which were considered as potentially contributing to the photoreaction due to their relatively large transition dipole moment from the electronic ground state (see [19] for more details). Bottom: The same plots including all excited states under consideration. In the molecular structure optimizations, all nuclear coordinates were allowed to relax except for the distance between the reactive carbon atoms, which was held fixed at the values indicated on the x axis (B3LYP-D3/ def-TZVP)

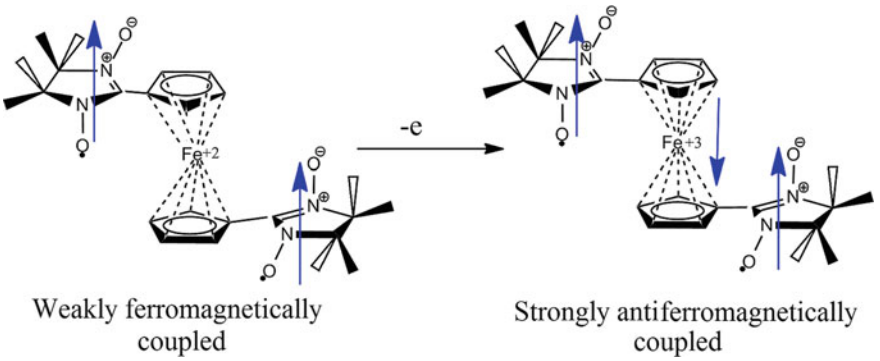

Fig. 6.9 Illustration of redox switching a bridging ferrocene unit linking two nitronyl nitroxide radicals to achieve an overall energetic stabilization of the ground state with respect to spin flips

coupled according to Kohn–Sham DFT. When oxidizing the bridge, the coupling between the spins on the radicals and on the bridge is antiferromagnetic, so that overall the relative orientation between the spins on the two radicals remains unchanged (i.e., aligned parallel). The resulting stabilization of the electronic ground state with respect to spin flips is at least by a factor of three (with some exchange–correlation functionals suggesting up to 300).

All these results were obtained from Kohn–Sham DFT (where it was verified that conclusions do not depend on the choice of a particular approximate exchange–correlation functional). It would be interesting to see whether this switching behavior can also be verified experimentally, and whether the stronger coupling in the oxidized state plays a role for adsorbates on surfaces (where oxidation may be caused by charge transfer form the molecule to the surface).

6.3.3 Introducing Spins on the Bridge: A Systematic Study

To study more systematically the effect of introducing a spin center on the bridge, we investigated a series of nitronyl nitroxide (NNO)–bridge–semiquinone (SQ) compounds, where the bridge is a *meta*-phenylene with different closed-shell and radical substituents (see Fig. 6.10) [73]. Again, introducing a spin on the bridge leads to an energetic stabilization of the ground state with respect to spin flips by a factor of three to six. There is a clear correlation between the amount of spin density that gets delocalized from the radical substituent onto the bridge and the amount of spin-state stabilization. Since in the potential synthetic target system (bottom right in Fig. 6.10), this delocalization is much smaller than in the model systems under study (the other panels in the figure), this points to controlling spin delocalization in synthetically accessible molecules as an important goal when aiming at a stabilization of coupled spin systems with respect to spin flips.

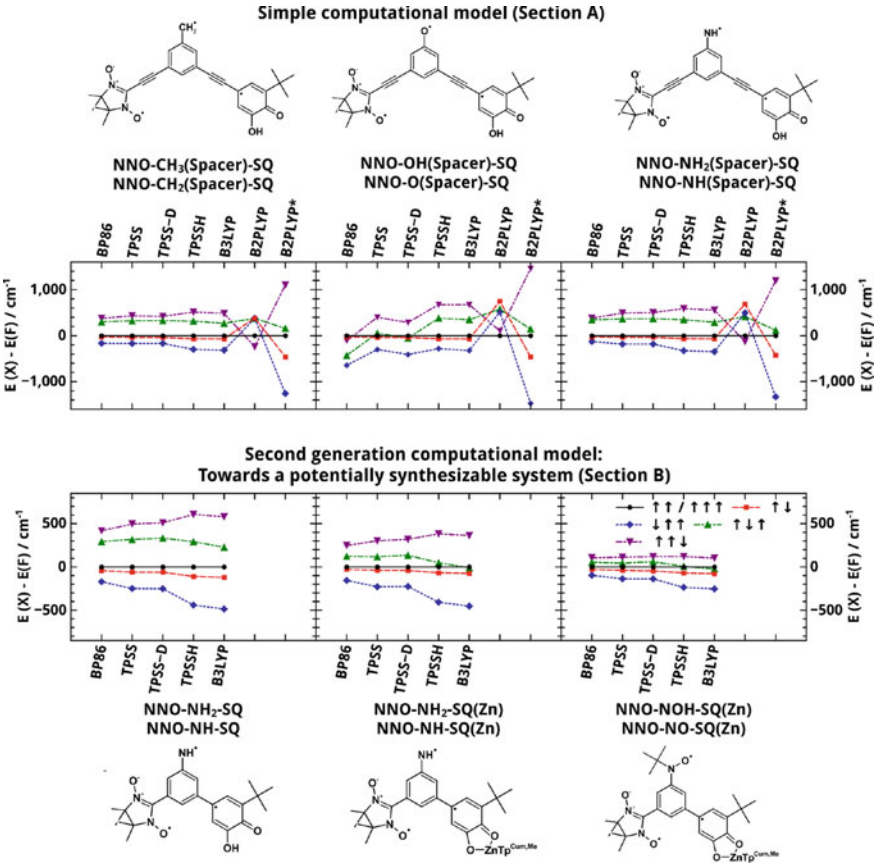

Fig. 6.10 (Top) Relative spin state energies of meta-connected ethynyl-bridged model radicals for different exchange–correlation functionals (legend: bottom right plot). (Bottom) Relative spin state energies of a potential synthetic target system. The Lewis structure shows structures with a radical substituent on the bridge, resulting in triradicals; these are compared with the spin-state energetics of analogous compounds with an added hydrogen atom changing the substituent into a closed-shell one, resulting in diradicals (compare the text below/above the Lewis structures). For both diradicals and triradicals, energies are given with respect to the ferromagnetically coupled state (↑↑ or ↑↑↑). B2PLYP* refers to the B2PLYP functional employing 100% DFT correlation rather than the original 27% admixture of MP2 correlation

6.4 From Spin Coupling to Conductance

The relation between spin coupling and electron transfer or transport has been studied for some time [24, 26–30]. Recently, it was also pointed out that there is a connection between the existence of diradicals and the occurrence of quantum interference in molecular wires [74]. We showed that comparing conductance and spin coupling from a molecular-orbital point of view results in the common trends reported before (with

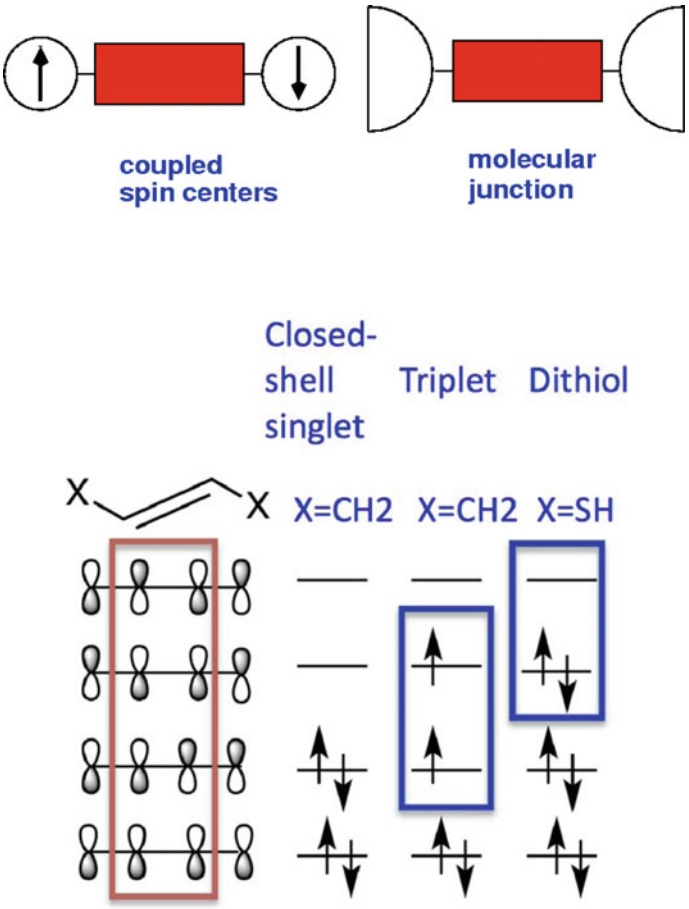

Fig. 6.11 Top: Schematic comparison of a molecular bridge (red rectangle) between two spin centers versus one between macroscopic electrodes (consisting, e.g., of gold with the bridge attached via thiolate linkers [75]). Bottom: Illustration of the frontier orbitals relevant for understanding spin coupling (middle) and molecular conductance (right). A larger energy splitting between the two singly occupied orbitals in the triplet diradical (blue box in middle molecular orbital scheme) indicates larger antiferromagnetic coupling, and a larger splitting between the two frontier orbitals in a molecular dithiolate bridge (blue box in the right-hand orbital scheme) indicates smaller conductance

large conductance corresponding to large antiferromagnetic coupling), but this is due to pairs of frontier orbitals showing opposite trends (see Fig. 6.11): Antiferromagnetic coupling gets larger as orbital energy splittings increase, while conductance gets smaller in that case (provided the electronic coupling to the electrodes remains the same). This apparent contradiction is explained by the fact that in a typical thiolate–bridge–thiolate molecular wire, there are two relevant electrons more than for a typical spin–bridge–spin system, so the relevant frontier orbitals are different [25].

We also studied radical and closed-shell adsorbates on carbon nanotubes, where they may affect conductance [76]. This effect is often called chemical gating, and it is attributed to charge transfer between adsorbates and nanotube, the effect of the adsorbate dipole moments on the nanotube electronic structure, or a combination of both. Therefore, this study required the derivation and implementation of a generalized origin-independent approach to evaluating local dipole moments [36, 37] (see Fig. 6.12).

When considering the relation between conductance and spin-dependent properties, other exciting phenomena are magnetoresistance [77] and effects resulting from spin–orbit coupling, such as the Rashba effect which in colloidal PbS nanosheets leads to a circularity dependent photo-galvanic effect [78]. For the magnetoresistance measured for a TEMPO-radical-substituted oligophenylene-ethynylene (OPE) molecular wire in a mechanically controlled break junction, electron transport does not go through the radical substituent (see Fig. 6.13), but yet the presence of the radical strongly increases magnetoresistance compared with the unsubstituted OPE molecule. This leaves several open questions for future work.

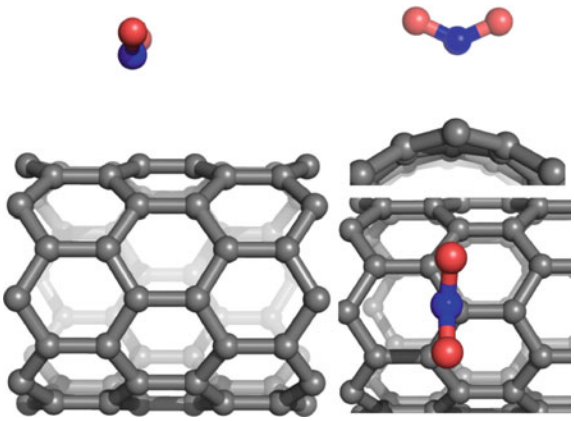

Fig. 6.12 Optimized structure of a spin-polarized NO_2 adsorbate on a (8,0) carbon nanotube (periodic boundary conditions, PBE-D2) [76]

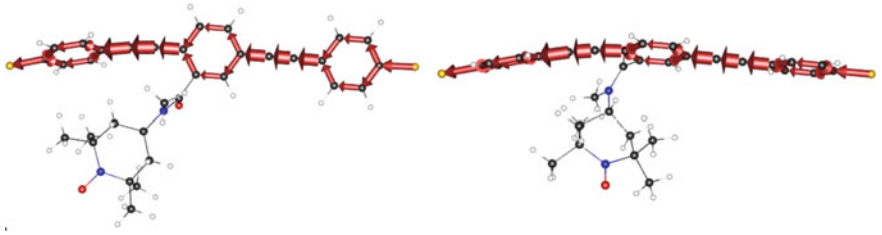

Fig. 6.13 Schematic illustration of local contributions to electron transmission in two nearly degenerate conformations of a TEMPO-substituted oligophenylene-ethynylene molecular wire [39, 77]

6.5 Conclusion

We have reviewed methodological and computational efforts towards understanding and designing spin interactions in molecular systems, which may be important for functional units in nanoscale spintronics. In particular, our focus was on analyzing local contributions to spin coupling (i.e., coupling pathways), on photoswitching and redoxswitching spin coupling, on quantifying the effect of unpaired spins located on bridging units, on the stabilization of the ground state with respect to spin flips, and on pointing out common aspects of spin coupling and conductance through molecular bridges. In the future, it would be valuable to employ the concepts and methods suggested here to specifically design (switchable) spin coupling in molecules and molecular chains, both isolated and on surfaces or in other environments that may facilitate their use for nanospintronics applications.

Acknowledgements For funding, we thank the DFG via SFB 668 (project B17). We are grateful for the support by and discussions with our collaborators within the SFB 668 and beyond, in particular Jürgen Heck, Alexander Lichtenstein, Elke Scheer, Christian Klinke, Martin L. Kirk, David A. Shultz, and their groups. Furthermore, we thank all Ph.D., master and bachelor students who have contributed to this project during the last years, in particular: Marc Philipp Bahlke, Martin Sebastian Zöllner, Joscha Nehrkorn, Conrad Stork, Aaron Bahde, Mariana Hildebrandt, Jos Tasche, Jonny Proppe, Jan Elmisz, Lea Freudenstein, Lawrence Rybakowski. We also gratefully acknowledge administrative support by Andrea Beese, Heiko Fuchs, and Beate Susemihl, and IT support and computing power by HLRN, the HPC cluster and team at the Regional Computing Center at University of Hamburg, and the chemistry IT service at University of Hamburg.

References

1. M.M. Waldrop, Nature **530**, 144 (2016)
2. A.A. Khajetoorians, B. Chilian, J. Wiebe, R. Wiesendanger, Science **332**, 1062 (2011)
3. A. DiLullo, S.H. Chang, N. Baadji, K. Clark, J.P. Klöckner, M.H. Prosenc, S. Sanvito, R. Wiesendanger, G. Hoffmann, S.W. Hla, Nano Lett. **12**, 3174 (2012)
4. M. Bazarnik, B. Bugenhagen, M. Elsebach, E. Sierda, A. Frank, M.H. Prosenc, R. Wiesendanger, Nano Lett. **16**(1), 577 (2016)
5. E. Sierda, M. Abadia, J. Brede, M. Elsebach, B. Bugenhagen, M.H. Prosenc, M. Bazarnik, R. Wiesendanger, ACS Nano. (2017)
6. J. Girovsky, J. Nowakowski, M.E. Ali2, M. Baljozovic, H.R. Rossmann, T. Nijs, E.A. Aeby, S. Nowakowska, D. Siewert, G. Srivastava, C. Wäckerlin, J. Dreiser, S. Decurtins, S.X. Liu, P.M. Oppeneer, T.A. Jung, N. Ballav, Nat. Commun. **8**, 15388 (2017)
7. M. Garnica, D. Stradi, S. Barja, F. Calleja, C. Diaz, M. Alcami, N. Martin, A.L.V. de Parga, F. Martin, R. Miranda, Nat. Phys. **9**, 368 (2013)
8. T. Steenbock, C. Herrmann, J. Comput. Chem. (2017). Accepted
9. A.I. Liechtenstein, M.I. Katsnelson, V.P. Antropov, V.A. Gubanov, J. Magn. Magn. Mater. **67**, 65 (1987)
10. D.W. Boukhvalov, V.V. Dobrovitski, M.I. Katsnelson, A.I. Lichtenstein, B.N. Harmon, P. Kögerler, Phys. Rev. B **70**, 054417 (2004)
11. D.W. Boukhvalov, A.I. Lichtenstein, V.V. Dobrovitski, M.I. Katsnelson, B.N. Harmon, V.V. Mazurenko, V.I. Anisimov, Phys. Rev. B **65**, 184435 (2002)
12. M. Han, T. Ozaki, J. Yu, Phys. Rev. B **70**, 184421 (2004)

13. T. Steenbock, J. Tasche, A. Lichtenstein, C. Herrmann, J. Chem. Theory Comput. **11**, 56515664 (2015)
14. K. Matsuda, M. Irie, J. Am. Chem. Soc. **122**, 7195 (2000)
15. K. Matsuda, M. Irie, Chem. Eur. J. **7**, 3466 (2001)
16. K. Takayama, K. Matsuda, M. Irie, Chem. Eur. J. **9**, 5605 (2003)
17. S. Nakatsuji, Chem. Soc. Rev. **33**, 348 (2004)
18. W.R.B. Ben L. Feringa, *Molecular Switches* (Wiley VCH, Hoboken, 2007)
19. A. Escribano, T. Steenbock, C. Stork, C. Herrmann, J. Heck, Chem. Phys. Chem. **18**, 596 (2017)
20. A. Ito, R. Kurata, D. Sakamaki, S. Yano, Y. Kono, Y. Nakano, K. Furukawa, T. Kato, K. Tanaka, J. Phys. Chem. A **117**, 12858 (2013)
21. M.E. Ali, V. Staemmler, F. Illas, P.M. Oppeneer, J. Chem. Theor. Comput. **9**, 5216 (2013)
22. E.D. Piazza, A. Merhi, L. Norel, S. Choua, P. Turek, S. Rigaut, Inorg. Chem. **54**, 6347 (2015)
23. S. Demir, I.R. Jeon, J.R. Long, T.D. Harris, Coord. Chem. Rev. **289**, 149 (2015)
24. C. Herrmann, J. Elmisz, Chem. Commun. **49**, 10456 (2013)
25. J. Proppe, C. Herrmann, J. Comput. Chem. **36**, 201 (2015)
26. M.L. Kirk, D.A. Shultz, E.C. Depperman, C.L. Brannen, J. Am. Chem. Soc. **129**, 1937 (2007)
27. M.L. Kirk, D.A. Shultz, D.E. Stasiw, G.F. Lewis, G. Wang, C.L. Brannen, R.D. Sommer, P.D. Boyle, J. Am. Chem. Soc. **135**(45), 17144 (2013)
28. G. Blondin, J.J. Girerd, Chem. Rev. **90**, 1359 (1990)
29. P. Bertrand, Chem. Phys. Lett. **113**(1), 104 (1985)
30. T.C. Brunold, D.R. Gamelin, E.I. Solomon, J. Am. Chem. Soc. **122**, 8511 (2000)
31. A.E. Clark, E.R. Davidson, Int. J. Quantum Chem. **93**, 384 (2003)
32. S.M. Bachrach, in *Reviews in Computational Chemistry*, vol. 5, ed. by K.B. Lipkowitz, D.B. Boyd (VCH Publishers, New York, 1994)
33. A.E. Clark, E.R. Davidson, J. Chem. Phys. **115**(16), 7382 (2001)
34. C. Herrmann, M. Reiher, B.A. Hess, J. Chem. Phys. **122**, 034102 (2005)
35. E. Ramos-Cordoba, E. Matito, I. Mayer, P. Salvador, J. Chem. Theory Comput. **8**, 1270 (2012)
36. L. Groß, C. Herrmann, J. Comput. Chem. **37**, 2324 (2016)
37. L. Groß, C. Herrmann, J. Comput. Chem. **37**, 2260 (2016)
38. A. Krawczuk, D. Prez, P. Macchi, J. Appl. Cryst. **47**, 1452 (2014)
39. G.C. Solomon, C. Herrmann, T. Hansen, V. Mujica, M.A. Ratner, Nat. Chem. **2**, 223 (2010)
40. T.H.T. Hansen, G.C. Solomon, J. Chem. Phys. **146**, 092322 (2017)
41. N. Sai, N. Bushong, R. Hatcher, M. di Ventra, Phys. Rev. B **75**, 15410 (2007)
42. M. Ernzerhof, J. Chem. Phys. **125**, 124104 (2006)
43. T.N. Todorov, J. Phys.: Condens. Matter **14**, 3049 (2002)
44. A. Pecchia, A.D. Carlo, Rep. Prog. Phys. **67**, 1497 (2004)
45. V. Pohl, L.E.M. Steinkasserer, J.C. Tremblay, arXiv:1707.07635
46. J.N. Onuchic, D.N. Beratan, J.R. Winkler, H.B. Gray, Ann. Rev. Biophys. Biomol. Struct. **21**, 349 (1992)
47. W. Hug, Chem. Phys. **264**, 53 (2001)
48. C. Herrmann, K. Ruud, M. Reiher, Chem. Phys. **343**, 200 (2008)
49. M.U. Delgado-Jaime, S. DeBeer, M. Bauer, Chem. Eur. J. **19**, 15888 (2013)
50. S.W. Oung, J. Rudolph, C.R. Jacob, Int. J. Quantum Chem. (2017)
51. J.E. Peralta, V. Barone, J. Chem. Phys. **129**, 194107 (2008)
52. J.J. Philips, J.E. Peralta, J. Chem. Phys. **138**, 174115 (2013)
53. P.O. Löwdin, J. Chem. Phys. **18**(3), 365 (1950)
54. G. Bruhn, E.R. Davidson, I. Mayer, A.E. Clark, Int. J. Quantum Chem. **106**, 2065 (2006)
55. L. Noodleman, J. Chem. Phys. **74**(10), 5737 (1981)
56. E. Ruiz, J. Cano, S. Alvarez, P. Alemany, J. Comput. Chem. **20**, 1391 (1999)
57. I. de P. R. Moreira, F. Illas, Phys. Chem. Chem. Phys. **8**, 1645 (2006)
58. J. Perdew, A. Savin, K. Burke, Phys. Rev. A **51**, 4531 (1995)
59. C. Jacob, M. Reiher, Int. J. Quantum Chem. **112**, 3661 (2012)
60. A.J. Cohen, D.J. Tozer, N.C. Handy, J. Chem. Phys. **126**, 214104 (2007)

61. J. Wang, A.D. Becke, V.H. Smith Jr., J. Chem. Phys. **102**(8), 3477 (1995)
62. C.J. Cramer, D.G. Truhlar, Phys. Chem. Chem. Phys. **11**, 10757 (2009)
63. A.P. Gingsberg, Inorg Chim. Acta Rev. **5**, 45 (1971)
64. N. Pagels, O. Albrecht, D. Görlitz, A.Y. Rogachev, M.H. Prosenc, J. Heck, Chem. Eur. J. **17**, 4166 (2011)
65. Y.O. Kvashnin, R. Cardias, A. Szilva, I. Di Marco, M. Katsnelson, A. Lichtenstein, L. Nordström, A. Klautau, O. Eriksson, Phys. Rev. Lett. **116**(21), 217202 (2016)
66. D.M. Korotin, V. Mazurenko, V. Anisimov, S. Streltsov, Phys. Rev. B **91**(22), 224405 (2015)
67. M. Deffner, L. Groß, T. Steenbock, B.A. Voigt, M.S. Zöllner, G.C. Solomon, C. Herrmann (2008–2017)
68. S. Trtica, M.H. Prosenc, M. Schmidt, J. Heck, O. Albrecht, D. Grlitz, F. Reuter, E. Rentschler, Inorg. Chem. **49**, 1667 (2010)
69. S. Puhl, T. Steenbock, R. Harms, C. Herrmann, J. Heck, Dalton Trans. (2017). (Under revision)
70. M. Irie, T. Fukaminato, K. Matsuda, S. Kobatake, Chem. Rev. **114**, 12174 (2014)
71. T. Steenbock, A. Escribano, J. Heck, C. Herrmann, Chem. Phys. Chem. **16**, 1491 (2015)
72. A. Escribano, T. Steenbock, C. Herrmann, J. Heck, Chem. Phys. Chem. **17**, 1881 (2016)
73. T. Steenbock, D.A. Shultz, M.L. Kirk, C. Herrmann, J. Phys. Chem. A **121**, 216 (2017)
74. Y. Tsuji, R. Hoffmann, M. Strange, G.C. Solomon, Proc. Natl. Acad. Sci. **113**(4), E413 (2016)
75. J.C. Cuevas, E. Scheer, *Molecular Electronics: An Introduction to Theory and Experiment*. World Scientific Series in Nanotechnology and Nanoscience, vol. 1 (World Scientific, Singapore, 2010)
76. L. Groß, M.P. Bahlke, T. Steenbock, C. Klinke, C. Herrmann, J. Comput. Chem. **38**, 861 (2017)
77. R. Hayakawa, M.A. Karimi, J. Wolf, T. Huhn, M.S. Zöllner, C. Herrmann, E. Scheer, Nano Lett. **16**, 4960 (2016)
78. M.M.R. Moayed, T. Bielewicz, M.S. Zöllner, C. Herrmann, C. Klinke, Nat. Commun. **8**, 15721 (2017)